Impact Factor:					
	ISRA (India) = 6.317	SIS (USA) = 0.912	ICV (Poland) = 6.630
	ISI (Dubai, UAE) = 1.582	РИНЦ (Russia) = 3.939	PIF (India) = 1.940
	GIF (Australia) = 0.564	ESJI (KZ) = 8.771	IBI (India) = 4.260
	JIF = 1.500	SJIF (Morocco) = 7.184	OAJI (USA) = 0.350

SOI: 1.1/TAS DOI: 10.15863/TAS

International Scientific Journal

Theoretical & Applied Science

p-ISSN: 2308-4944 (print) **e-ISSN:** 2409-0085 (online)

Year: 2023 **Issue:** 11 **Volume:** 127

Published: 23.11.2023 **http://T-Science.org**

Issue Article

Mikhail Aleksandrovich Frolov
Samara State Technical University
Senior Lecturer

MECHANICAL PROPERTIES OF POROUS MATERIAL BASED ON TRIPLY PERIODIC SURFACES OBTAINED FROM THE ATOMIC NETWORK OF SODALITE

Abstract: *Mechanical properties of porous material based on triply periodic surface are explored experimentally and theoretically. The triply periodic surfaces (TPS) are obtained by new method on the basis of a topological network representation of the crystal structures of chemical compounds. A model of a porous material based on the crystalline structure of sodalite has been created, samples of the material are manufactured using 3D printing, their mechanical properties are studied using computer-aided design and measured experimentally. The simulation results are in good agreement with the experiment and previous works on schwarzide-p.*

Key words: *triply periodic surfaces, additive manufacturing, scaffold material, compression stiffness, compression modulus, Mises stress, Gibson-Ashby model.*

Language: *English*

Citation: Frolov, M. A. (2023). Mechanical properties of porous material based on triply periodic surfaces obtained from the atomic network of sodalite. *ISJ Theoretical & Applied Science, 11 (127),* 267-273.

Soi: http://s-o-i.org/1.1/TAS-11-127-33 ***Doi***: https://dx.doi.org/10.15863/TAS.2023.11.127.33

Scopus ASCC: *2200.*

Introduction

UDC 620.173.22

Modern technologies widely use materials with porous structure of various types and dimensions [1]. An important group of such materials, which attracted attention in the last years, is based on smooth triply periodic surfaces (TPS) with diverse topological and geometrical structure [2, 3]. The interest to these materials is primarily caused by their thermal-conductive, electrical-conductive, acoustic, and vibration-isolating properties [4, 5], as well as by their ability to adsorb strain energy [6-11]. Filling pores with the materials to be different from the skeleton base material enables one to fabricate new composite materials and metamaterials with wide range and considerable anisotropy of physical properties. The mentioned features together with the Additive Manufacturing (AM) technology make the TPS materials an indispensable part of modern engineering solutions and thus are a subject of intense theoretical and experimental studies.

As is known, the number of TPS currently used in the development of porous materials is very limited, and the task of creating new TPS is an urgent scientific task [12]. In this article, we test a new method for obtaining porous materials based on TPS, based on a topological network representation of the crystal structures of chemical compounds, in particular zeolites [13, 14]. The theoretical foundations of this method are described in detail in [15]. This approach makes it possible to generate an unlimited number of TPSs and corresponding porous materials using the ToposPro software package [16]. After a certain thickness is given to the surface, it can be printed as a part by additive manufacturing, and its physical properties can be investigated using a computer-aided engineering (CAE) systems, such as the ANSYS software [17], and studied experimentally. As an example, we generated a model of a porous material from the crystal structure of a zeolite-type sodalite and produced 3D-printed samples of various shapes and sizes from a styrene butadiene copolymer (SBS). We measured the mechanical characteristics of cylindrical porous SBS samples and found that they perfectly match the parameters modeled using the ANSYS software.

The structure of the article is as follows. Section 2 describes experimental measurement of mechanical properties of porous structure. In Section 3 the numerical modeling of mechanical properties and comparison of the results with experimental data is produced. In conclusion, the main results of the work done are summarized.

2. Experimental investigation of mechanical properties of SOD-based TPS-based porous structures

To study the mechanical properties of a SOD-based material porous right circular cylinders with a diameter of 30 mm and a height of 60 mm were manufactured by SBS 3D printing. The cylinders consisted of elementary SOD-based RVEs with wall thickness of 0.2 mm, which can be inscribed in cubes with edges of 8.89 mm. Each cylinder was based on a layer of 36 RVEs joined in a horizontal plane, and there were 12 such layers in the cylinder (Fig. 1).

Figure 1. Sample of SOD-based TPS-based porous structure manufactured by 3D printing FDM technology.

Mechanical properties of the samples manufactured from SBS significantly depend on the 3D printing mode, in particular, on the fiber-laying direction. In this regard, before studying porous samples, it is necessary to experimentally measure the mechanical characteristics of the SBS material after passing through the 3D printer. For this purpose, several solid cylinders of the above-mentioned dimensions were manufactured on the same printer using the same technology.

Measurement of the mechanical characteristics of all samples was carried out on a SHIMADZU tensile testing machine, which allows recording measurement results in an automatic mode. Compression of samples was performed at a rate of 1 mm/min. The error of all measurements did not exceed 0.01%.

The experimental stress-strain curve averaged for all solid examples (Fig. 2) revealed linear increase of strain at low stress and plastic strain area up to the stress of 17,4 MPa. This behavior is typical for such materials [18].

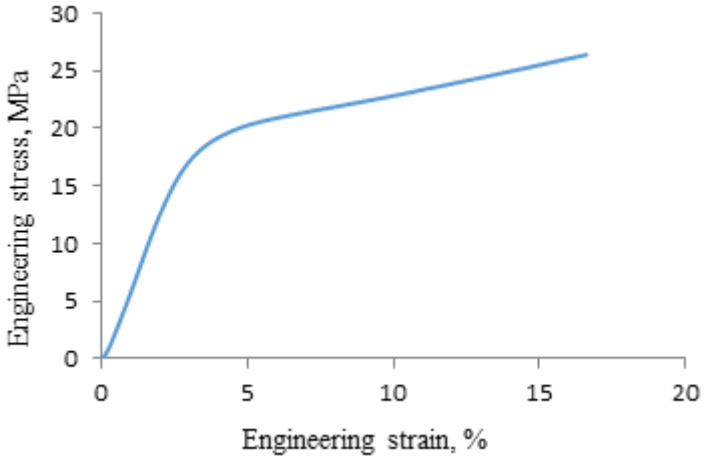

Figure 2. Averaged experimental stress-strain curve during compression of solid cylinders manufactured from SBS by the FDM technology.

Further the so-called cold flow was observed, i.e. the growth of strain occured at a slightly increasing stress up to 26 MPa. This region is characterized by the absence of a yield point, which apparently indicates a change in the supramolecular structure of the polymer. Using the experimental data presented in Fig. 11 we estimated the mean value of the elastic compression modulus as E = 625.6 MPa in the range ε= 1 – 3%. The obtained value is within the allowable range of this modulus for the SBS polymer at room temperature.

Porous samples (Fig. 1) were studied using the same experimental technique as solid samples. The averaged experimental loading curve (Fig. 3a) revealed three stages that the porous samples passed through before being compressed into a solid disk. The first area (ε=0–1%) is linear with a gradual predominance of plastic strain over elastic strain, while slip planes are gradually formed on the sample (Fig. 3b). This behavior of the sample is preserved up to $\varepsilon\approx$3%. The second part of the curve (ε=1–2%) contains a maximum, which is apparently caused by the strain of the RVEs along the slip planes (Fig. 3c)).

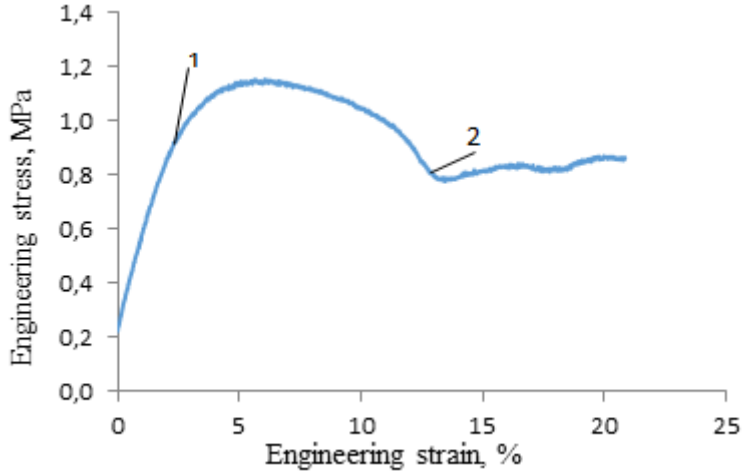

a)

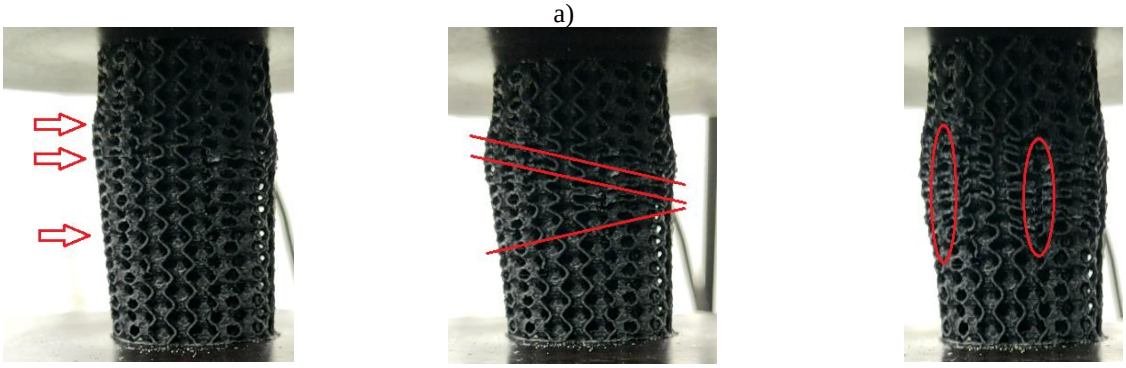

b) c) d)

Figure 3. a) is averaged loading curve of the porous samples; b) is the first (elastic) stage of strain (ε=0–1%), c) is the second stage of strain (diagonal slip area, ε=1–2%), d) is the third stage of strain (second yield area, ε=2%–failure). The arrows indicate the emerging slip planes.

In the third part (Fig. 3d) longitudinal cracks were formed in the volume of the samples under tensile stresses perpendicular to the compress direction. All three stages of the sample compression are characterized by the lack of symmetry in the formation of slip planes and their further propagation, in crack formation, as well as in compression of RVEs. Apparently, these features are the consequences of the anisotropy that is caused by the selected 3D printing mode, as well as by the printing quality. Note that the resulting loading curve (Fig. 3a) is quite typical for porous materials based on three-periodic surfaces [1].

The elastic compression modulus E_c was determined by averaging the values of the curve slope within ε=1–2% (Fig. 3a):

$$E_c = (22.41\pm2.23)\ \text{MPa} \quad (1)$$

3. Theoretical investigation of mechanical properties of SOD-based TPS-based porous structures

The finite element method implemented in the ANSYS was used for the computer modelling of the experimental on measurement of the elastic properties of porous samples, as well as for predicting their mechanical properties when changing their size, shape and the RVE thickness. At the first step, we selected the most suitable model for describing the nonlinear mechanical properties of the material. According to its mechanical properties, the SBS polymer belongs to the class of hard rubbers, i.e., the Poisson ratio of this material is close to 0.5. Such rubber-like materials are generally considered to be hyperelastic and can experience large elastic and viscoplastic strains. To simulate the mechanical properties of samples made from such materials Green's model of hyperelastic material is used as a rule [19].

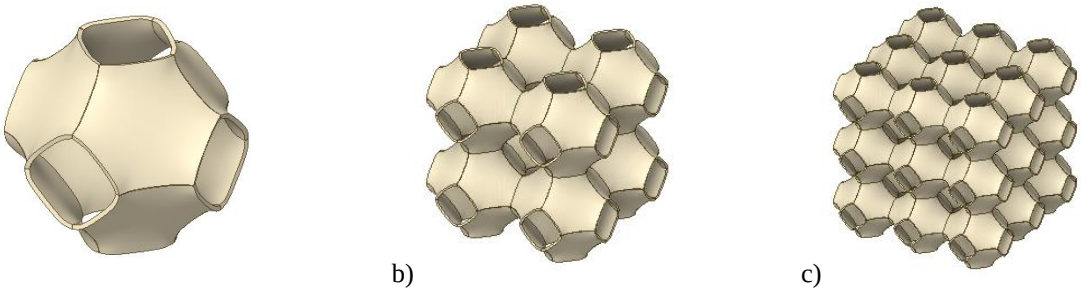

a) b) c)

Figure 4. Objects with 1 a), 8 b) and 27 c) SOD-based unit cells, for which the calculations of the modulus of elastic compression and the shear modulus were performed.

Calculations of the mechanical properties of porous samples in this model require analytical fitting of the experimental loading curve for solid cylinders (Fig. 2). We performed such fitting in ANSYS using the Yeoh model [20]. In these frameworks the mechanical properties of simple objects with the number of RVEs 1, 8 and 27 (Fig. 4) were first modeled. The values of corresponding elastic constants for a given RVEs are presented Table 1.

Table 1. Modulus of elastic compression E_c and shear modulus G for porous objects with different number of RVE and thickness of walls (Fig. 4).

Number of RVEs in layers length	Thickness of walls, mm		
	0.06	0.08	0.20
	E_c, MPa	E_c, MPa	E_c, MPa
1	1.13	1.51	2.01
2	2.26	3.02	3.78
3	3.39	4.53	4.38

The finite element model was constructed using the patch-controlled method, with additive mesh for in-depth detailing of stresses at the places of application of the load and sealing of a geometric object. All finite elements were linear tetrahedral elements with reduced integration; type SOLID 185, according to the ANSYS labeling scheme (Fig. 5a). Quality of mesh confirmed by Jacobian of constructed finite element model (Fig. 5b).

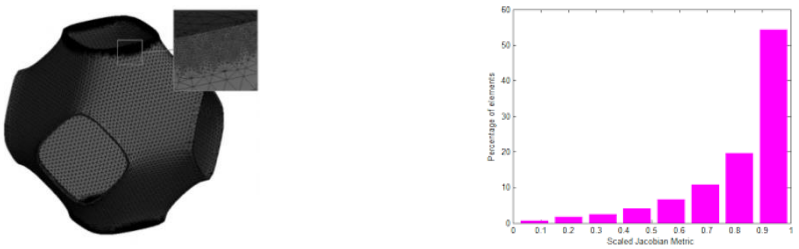

a) b)

Figure 5. Finite element model of SOD-based material. a) show the details of the place of application of the load, b) is the Jacobi matrix of the resulting finite element model.

Constructed finite element model was solved using Dirichlet boundary conditions:

$$\Delta\varphi(u_1) = 0, \quad \forall u_1 \in \Omega, \tag{2}$$

$$\varphi(u_1) = f(u_1), \quad \forall u_1 \in \partial\Omega, \tag{3}$$

where φ is the unknown function, u_1 is the independent displacement (e.g. the spatial coordinates), Ω is the function domain, ∂Ω is the boundary of the domain, and f is a given scalar function defined on ∂Ω (Fig. 6).

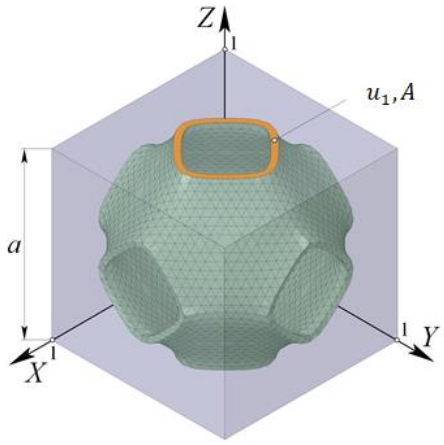

Figure 6. RVE-scheme of boundary condition of SOD-based surface.

The values of the compression module were obtained using well-known dependencies:

$$E_c = \frac{\sigma}{\varepsilon_c}, \tag{4}$$

$$\sigma = \frac{F}{A} \tag{5}$$

$$\varepsilon_c = \frac{a - a_c}{a}\,100\% \tag{6}$$

where E_c is compression modulus, σ is compression stress, ε_c is compression strain, F is force acting on surface, A is area of surface, a is initial length, a_c is compressed length.

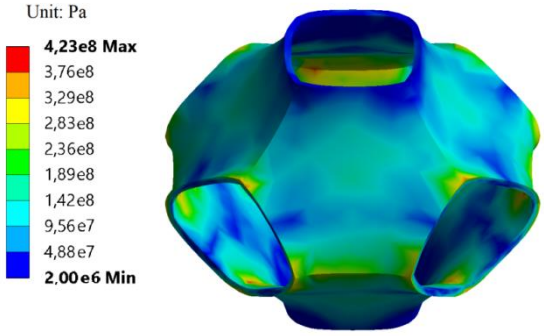

Figure 7. Von Mises stress distribution under compression in a SOD-based RVE sample.

The von Mises stress distribution (Fig. 7) is quite uniform and slightly varies close to 142 MPa. Such a uniform distribution is typical for triply periodic minimal surfaces [21], which equivalent to our SOD-based surface. The high uniformity of stress distribution in our porous sample confirms that the smoothing procedure described in Section 2 includes the condition and, hence, results in a minimal mean curvature of the surface, or in the limit to zero mean curvature, i.e. to a minimal surface. However, in the sample in Fig. 7 there are small border areas where the stress differs significantly from the average value and reaches 423 MPa.

Note that the direct calculation of the mechanical properties of samples with a large number of RBEs and, in particular, the experimentally studied 3D printed cylinder (Fig. 3) is resource-consuming due to the topological and geometric complexity of the object. In this regard, we say that the dependence of the compression modulus in Table 2 on the number of horizontal layers in the sample is close to linear. We performed a rough linear extrapolation over three points and calculated a confidence interval with a confidence probability of 0.7 for the compression modulus at the number of layers equal to 12, i.e. at the number of layers in the cylinder. The experimental value of the compression modulus (4) for the cylinder is within the obtained confidence interval.

Our calculations are compared with calculations of the mechanical characteristics of porous structures

performed in other works. For this purpose, the results for the elastic modulus presented in Table 2 were converted in a function of the average density of the porous structure. The thus obtained function was placed on the Ashby diagram (Fig. 8). The diagram shows for comparison the results for other porous structures from Ref. [21].

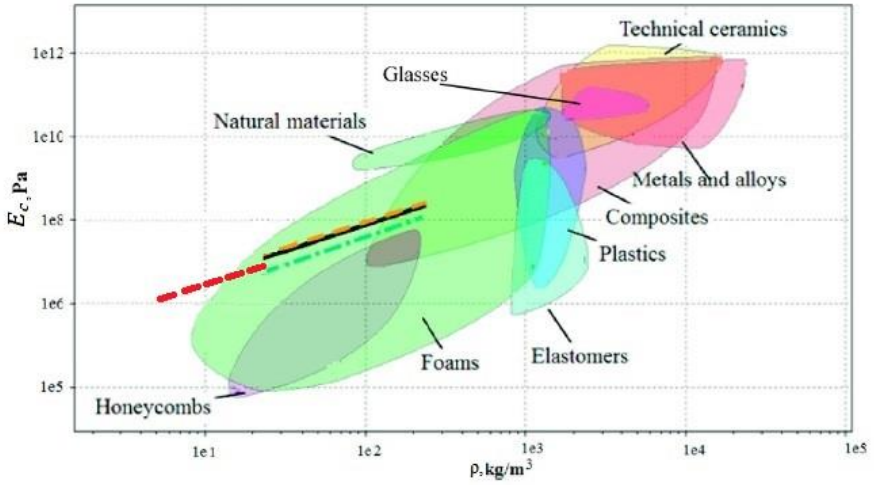

Figure 8. Ashby diagram with porous materials [21]. Black solid, yellow dashed and green dashed-dotted lines correspond to Neovius, IWP and P surfaces; dashed red line is the results of our study for the SOD-based surface.

The dependence of E_c on the average density of our porous structures (Fig. 8) is linear as for porous materials studied by other authors [21] including the ideal *P* surface, and follows these dependencies. An insignificant difference in the dependencies is apparently caused by the difference in the materials, from which the porous structures were fabricated, as well as in the selected 3D printing mode.

Conclusion

A porous structure was generated from sodalite crystal by new method on the basis of a topological network representation of the crystal structures of chemical compounds. Samples of this material were manufactured by 3D printing from SBS filament, and investigation of their thermal and mechanical properties was conducted. Experimental studies of samples obtained by 3D printing were carried out in the work in order to verify theoretical models. A very good agreement between theoretical calculations and experiment was obtained.

Experimental measurements of mechanical properties for porous samples in the form of right circular cylinders were made. Experimental loading curve was obtained, and compression modulus for these porous objects was measured. Loading curve was obtained and elastic compression modulus for these porous objects was measured in experiments.

Numerical modeling of mechanical properties for porous objects was performed. We calculated elastic compression modulus for various relative densities of the porous samples. The results for compression modulus thus obtained fall on Ashby diagram very close to the respective results obtained for porous structures in other studies.

So, the results obtained in the present paper give opportunity to state high efficiency and great opportunities of the suggested approach to generation of new porous materials as well as in theoretical and experimental studies of their mechanical properties.

Acknowledgement

The research was supported by the Russian Science Foundation (grant No. 22-23-00300, https://rscf.ru/project/22-23-00300/).

References:

1. Gibson, L. J., & Ashby, M. F. (2014). *Cellular Solids: Structure and Properties.* Cambridge University Press, 2014. doi: 10.1017/CBO9781139878326.

2. Villani, C. (2009). *Optimal transport: old and new*. Grundlehren der mathematischen Wissenschaften, Springer-Verlag Berlin 2009; 338.
3. Ashby, M. F., et al. (2002). Metal Foams: a Design Guide. *Materials and Design*; Feb.2002; 23: 119. doi: 10.1016/S0261-3069(01)00049-8.
4. Abueidda, D. W., Abu Al-Rub, R. K., Dalaq, A. S., Lee, D. W., Khan, K. A., & Jasiuk, I. (2016). Effective conductivities and elastic moduli of novel frames with triply periodic minimal surfaces. *Mech. Mater*. Apr.2016; 95: 102-115. doi:10.1016/j. mechmat.2016.01.004.
5. Abueidda, D. W., Dalaq, A. S., Abu Al-Rub, R. K., & Jasiuk, I. (2015). Micromechanical finite element predictions of a reduced coefficient of thermal expansion for 3D periodic architectured interpenetrating phase composites. *Compos. Struct.* Dec. 2015; 133: 85-97. doi: 10.1016/j.compstruct. 2015.06.082.
6. Maskery, I., et al. (2017). Insights into the mechanical properties of several triply periodic minimal surface lattice structures made by polymer additive manufacturing. *Polymer* (Guildf) Sep. 2018; 152: 62-71. doi: 10.1016/j.polymer.2017.11.049.
7. Montazerian, H., Davoodi, E., Asadi-Eydivand, M., Kadkhodapour, J., & Solati-Hashjin, M. (2017). Porous scaffold internal architecture design based on minimal surfaces: A compromise between permeability and elastic properties. *Mater. Des.* Jul. 2017; 126: 98-114. doi: 10.1016/j.matdes.2017.04. 009.
8. Lee, D. W., Khan, K. A., & Abu Al-Rub, R. K. (2017). Stiffness and yield strength of architectured frames based on the Schwarz Primitive triply periodic minimal surface. *Int. J. Plast.* Aug. 2017; 95: 1-20. doi: 10.1016/j.ijplas.2017.03.005.
9. Panesar, A., Abdi, M., Hickman, D., & Ashcroft, I. (2017). Strategies for functionally graded lattice structures derived using topology optimisation for Additive Manufacturing. *Addit. Manuf.* Jan. 2018; 19: 81-94. doi: 10.1016/j.addma.2017.11.008.
10. Al-Ketan, O., Rowshan, R., & Abu Al-Rub, R. K. (2017). Topology-mechanical property relationship of 3D printed strut, skeletal, and sheet based periodic metallic cellular materials. *Addit. Manuf.* Jan. 2018; 19: 167-183. doi: 10.1016/j. addma.2017.12.006.
11. Downing, D., Jones, A., Brandt, M., & Leary, M. (2020). Increased efficiency gyroid structures by tailored material distribution. *Materials and Design* Jan. 2021; 197. doi.org/10.1016/j.matdes.2020. 109096.
12. Pérez, J. (2017). New Golden Age of Minimal Surfaces. *Not. Am. Math. Soc.* Apr. 2017; 64: 347-358. doi: http://dx.doi.org/10.1090/noti1500
13. Gebbink, B. K., & Rodriguez, J., Eds. (2017). *Zeolites in Catalysis Properties and Applications.* London UK: The Royal Society of Chemistry, 2017. doi: 10.1039/9781788010610-FP001.
14. Jiang, N., et al. (2019). The adsorption mechanisms of organic micropollutants on high-silica zeolites causing S-shaped adsorption isotherms: An experimental and Monte Carlo simulation study. *Chem. Eng. J.* Jun. 2020; 389: 123968. doi: 10. 1016/j.cej.2019.123968.
15. Smolkov, M. I., Blatova, O. A., Krutov, A. F., & Blatov, V. A. (2022). Generating triply periodic surfaces from crystal structures: the tiling approach and its application to zeolites. *Acta Cryst. A* Jul. 2022; 78: 327 - 336. doi: https://doi.org/10.1107/S2053273322004545
16. Blatov, V. A., Shevchenko, A. P., & Proserpio, D. M. (2014). Applied topological analysis of crystal structures with the program package ToposPro. *Cryst. Growth Des* May 2014; 14: 3576-3586. doi: Retrieved from https://doi.org/10.1021/cg500498k
17. Thompson, M. K., & Thompson, J. M. (2017). *ANSYS Mechanical APDL for Finite Element Analysis.* Oxford, UK: Elsevier Inc., 2017.
18. Shanks, R., & Kong, I. (2012). *Thermoplastic Elastomers, in Thermoplastic Elastomers, A. El-Sonbati, Ed.* London, UK: Intech Open, 2012, p.139. Retrieved from https://doi.org/10.5772/36807
19. Rivlin, R. S. (1997). *Some applications of elasticity theory to rubber engineering.* in Collected Papers of R. S. Rivlin, G. I. Barenblatt and D. D. Joseph, Eds. New York, NY, USA: Springer, 1997, pp. 9-16. Retrieved from https://doi.org/10.1007/978-1-4612-2416-7
20. Yeoh, O. H. (1993). *Some forms of the strain energy function for rubber.* Rubber Chem. and Tech. Nov. 1993; 66: 754-771. doi: https://doi.org/10.5254/1.3538343
21. Abueidda D. W., et al. (2017). Mechanical properties of 3D printed polymeric cellular materials with triply periodic minimal surface architectures. *Materials & Design* May 2017; 122: 255-267. https://doi.org/10.1016/j.matdes.2017.03.018.